

The First Stars and Galaxies – Basic Principles

V. Bromm

*University of Texas, Department of Astronomy, Austin, TX 78712,
U.S.A.*

Abstract. Understanding the formation of the first stars and galaxies is a key problem in modern cosmology. In these lecture notes, we will derive some of the basic physical principles underlying this emerging field. We will consider the basic cosmological context, the cooling and chemistry in primordial gas, the physics of gravitational instability, and the main properties of the first stars. We will conclude with a discussion of the observational signature of the first sources of light, to be probed with future telescopes, such as the *James Webb Space Telescope*.

1. Introduction

The first sources of light fundamentally transformed the early universe, from the simple initial state of the cosmic dark ages into one of ever-increasing complexity (for comprehensive reviews, see Barkana & Loeb 2001; Bromm et al. 2009; Loeb 2010; Whalen et al. 2010). This process began with the formation of the first stars, the so-called Population III (Pop III), at redshifts $z \sim 20 - 30$. These stars are predicted to form in dark matter minihalos, comprising total masses of $\sim 10^6 M_\odot$. Current models suggest that Pop III stars were typically massive, or even very massive, with $M_* \sim 10 - 100 M_\odot$; these models also predict that the first stars formed in small groups, including binaries or higher-order multiples. First star formation has been reviewed in Bromm & Larson (2004) and Glover (2005). There, you will find a survey of the key papers up to 2005. For the most recent developments, I recommend to consult the specialized literature (e.g., Turk et al. 2009; Stacy et al. 2010; Clark et al. 2011; Greif et al. 2011).

Once the first stars had formed, feedback processes began to modify the surrounding intergalactic medium (IGM). It is useful to classify them into 3 categories (see Ciardi & Ferrara 2005): radiative, mechanical, and chemical. The first feedback consists of the hydrogen-ionizing photons emitted by Pop III stars, as well as the less energetic, molecule-dissociating radiation in the Lyman-Werner (LW) bands. Once the first stars die, after their short life of a few million years, they will explode as a supernova (SN), or directly collapse into massive black holes (MBHs). In the SN case, mechanical and chemical feedback come into play. The SN blastwave exerts a direct, possibly very disruptive, feedback on its host system, whereas the chemical feedback acts in a more indirect way, as follows: The first stars, forming out of metal-free, primordial gas, are predicted to be characterized by a top-heavy initial mass function (IMF). Once the gas had been enriched to a threshold level, termed “critical metallicity” (Z_{crit}), the mode of star formation would revert to a more normal IMF, which is dominated by lower mass stars (see Frebel et al. 2007). Chemical feedback refers to this transition in star

formation mode, implying that less massive stars have a less disruptive impact on their surroundings. The complex physics of pre-galactic metal enrichment, and the nucleosynthesis in Pop III SNe, are reviewed in Karlsson et al. (2012).

The first, Pop III stars are thus predicted to form in small groups, in minihalos with shallow gravitational potential wells. As they were typically very massive, they would quickly exert a strong negative feedback on their host systems. Numerical simulations indicate that this feedback completely destroys the host, in the sense of heating and evacuating all remaining gas. There would therefore be no opportunity for a second burst of star formation in a minihalo. Furthermore, since all (most?) Pop III stars are massive enough to quickly die, there would be no long-lived system of low-mass stars left behind. The Pop III forming minihalos, therefore, are *not* galaxies, if a bona-fide galaxy is meant to imply a long-lived stellar system, embedded in a dark matter halo. The question: *What is a galaxy, and, more specifically, what is a first galaxy?*, however, is a matter of ongoing debate (see Bromm et al. 2009). And as we have seen, this question is intimately tied up with the feedback from the first stars, which in turn is governed by the Pop III IMF (top-heavy or normal).

Theorists are currently exploring the hypothesis that “atomic cooling halos” are viable hosts for the true first galaxies (Oh & Haiman 2002). These halos have deeper potential wells, compared to the minihalos mentioned above; indeed, they have ‘virial temperatures’ of $T_{\text{vir}} \simeq 10^4$ K, enabling the primordial gas to cool via efficient line emission from atomic hydrogen. We will further clarify these concepts below. It is useful to keep in mind that observers and theorists often employ different definitions. As a theorist, you wish to identify the first, i.e., lowest-mass, dark matter halos that satisfy the conditions for a galaxy. Observers, on the other hand, usually aim at detecting truly metal-free, primordial systems. Recent simulation results, however, suggest that such metal-free galaxies do not exist. The reason being that rapid SN enrichment from Pop III stars, formed in the galaxy’s minihalo progenitors, provided a bedrock of heavy elements. Any second generation stars would then already belong to Population II (Pop II). These questions, and the problem of first galaxy formation in general, have been reviewed in Bromm & Yoshida (2011), where the reader can again find pointers to the detailed literature. For a comprehensive overview of galaxy formation and evolution in general, including the situation at lower redshifts, $0 < z < 5$, see the monograph by Mo et al. (2010).

The first star and galaxy field is just entering a dynamic phase of rapid discovery. This development is primarily driven by new technology, on the theory side by ever more powerful supercomputers, reaching peta-scale machines, and on the observational side by next-generation telescopes and facilities. Among them are the *James Webb Space Telescope (JWST)*, planned for launch in ~ 2018 , and the suite of extremely large, ground-based telescopes, such as the GMT, TMT, and E-ELT. The capabilities of the *JWST* are summarized in Gardner et al. (2006), as well as in the monograph by Stiavelli (2009). Complementary to them are ongoing and future meter-wavelength radio arrays, designed to detect the redshifted 21cm radiation from the neutral hydrogen in the early universe (see the review by Furlanetto et al. 2006). A further intriguing window into the epoch of the first stars is provided by high-redshift gamma-ray bursts (GRBs). These are extremely bright, relativistic explosions, triggered when a rapidly rotating

massive star is collapsing into a black hole (see the monograph by Bloom 2011). The first stars are promising GRB progenitors, thus possibly enabling what has been termed “GRB cosmology” (for details see Kouveliotou et al. 2012).

There is a second approach to study the ancient past, nicely complementary to the *in situ* observation of high-redshift sources. This alternative channel, often termed “Near-Field Cosmology” (Freeman & Bland-Hawthorn 2002), is provided by local fossils that have survived since early cosmic times. Among them are extremely metal-poor stars found in the halo of the Milky Way. The idea here is to scrutinize their chemical abundance patterns and derive constraints on the properties of the first SNe, and, indirectly, of the Pop III progenitor stars, such as their mass and rate of rotation (for reviews, see Beers & Christlieb 2005; Frebel 2010). Another class of relic objects is made up of the newly discovered extremely faint dwarf galaxies in the Local Group. These ultra-faint dwarf (UFD) galaxies consist of only a few hundred stars, and reside in very low-mass dark matter halos. Their chemical and structural history is therefore much simpler than what is encountered in massive, mature galaxies, and it should be much more straightforward to make the connection with the primordial building blocks (e.g., Salvadori & Ferrara 2009).

The plan for these lecture notes is to provide a theoretical ‘toolkit’, containing the basic physical principles that are the foundation to understand the end of the cosmic dark ages. We will consider the overall cosmological context, the fundamentals of star formation as applicable to the primordial universe, the properties of the first stars, and the physical principles underlying the assembly of the first galaxies. We conclude with some useful tools of observational cosmology, allowing us to connect theory with empirical probes. For a detailed discussion of the phenomenology and the numerical simulations, we refer the reader to the review papers and monographs cited above. Again, the goal here is to focus on the basic framework, which will likely be relevant for many years to come, enabling the student to follow the rapid progress unfolding in the research literature. I invite you to join in on this grand journey of discovery!

2. The Cosmological Context

2.1. CDM Structure Formation

We now have a very successful model that describes the expansion history of the universe, and the early growth of density fluctuations (Komatsu et al. 2011). This is the Λ cold dark matter (Λ CDM) model, as calibrated to very high precision by the *Wilkinson Microwave Anisotropy Probe* (WMAP). Structure formation in this model proceeds hierarchically, in a bottom-up fashion, such that small objects emerge first, and subsequently grow through mergers with neighboring objects and the smooth accretion of matter. To characterize the resulting distribution of density fluctuations, we measure the “overdensity” in a spherical window of radius R and total (gas + dark matter) mass M , where $M = 4\pi/3\bar{\rho}R^3$:

$$\delta_M \equiv \frac{\rho - \bar{\rho}}{\bar{\rho}} . \quad (1)$$

Here, ρ is the mass density within a given window, and $\bar{\rho}$ that of the background universe at the time the overdensity is measured. Next, the idea is to place

the window at random everywhere in the universe, and to calculate the (mean-square) average: $\sigma^2(M) = \langle \delta_M^2 \rangle$, where the brackets indicate a spatial average. The latter is closely related to the ensemble average, where one considers many realizations of the underlying random process that generated the density fluctuations in the very early universe (ergodic theorem). Here and in the following, all spatial scales are physical, as opposed to comoving, unless noted otherwise.

Due to gravity, the density perturbations grow in time. This growth is described with a “growth factor”, $D(z)$, such that:

$$\sigma \propto D(z) \propto a = \frac{1}{1+z} . \quad (2)$$

The second proportionality is only approximate, and would be strictly valid in a simple Einstein-de Sitter background model. The expression for the growth factor is more complicated in a Λ -dominated universe (see Loeb 2010), but the Einstein-de Sitter scaling still gives a rough idea for what is going on at $z \gg 1$. Indeed, it is quite useful for quick back-of-the-envelope estimates. Early on, all fluctuations are very small, with $\delta_M \ll 1$; but at some point in time, a given overdensity will grow to order unity. One says that a fluctuation is in its linear stage, as long as $\delta_M < 1$, and becomes “non-linear” when $\delta_M > 1$. Formally, a critical overdensity of $\delta_c = 1.69$ is often used to characterize the transition. The behavior and evolution of the perturbations in their linear stage can be treated analytically, e.g., by decomposing a density field into Fourier modes. Once the fluctuation turns non-linear, one needs to resort to numerical simulations to further follow them to increasingly high densities.

A basic tenet of modern cosmology is that the quantum-mechanical processes that imprinted the density fluctuations in the very early universe left behind a (near-) Gaussian random field. The probability that an overdensity has a given value, around a narrow range $d\delta_M$ is then:

$$P(\delta_M)d\delta_M = \frac{1}{\sqrt{2\pi\sigma_M^2}} \exp \left[-\frac{\delta_M^2}{2\sigma_M^2} \right] d\delta_M . \quad (3)$$

One speaks of a “ ν -sigma peak”, when: $\delta_M = \nu\sigma_M$. Note that high-sigma peaks are increasingly unlikely, and therefore rare. One also says that such peaks are highly biased, and one can show that such peaks are strongly clustered (see, e.g., Mo et al. 2010). The sites for the formation of the first stars and galaxies are predicted to correspond to such high-sigma peaks. To predict the redshift of collapse, or “virialization” redshift (see below), we demand: $\delta_M(z) = D(z)\delta_M(z=0) \simeq \delta_c$, or, using equ. (2)

$$\frac{\nu\sigma_M(z=0)}{1+z_{\text{vir}}} \simeq 1.69 ,$$

such that: $1+z_{\text{vir}} \simeq \nu\sigma_M(z=0)/1.69$, where $\sigma_M(z=0)$ is the rms density fluctuation, extrapolated to the present. On the scale of a minihalo ($M \sim 10^6 M_\odot$), one has: $\sigma_M(z=0) \sim 10$. For collapse (virialization) to occur at, say, $z_{\text{vir}} \simeq 20$, we would then need $\nu \simeq 3.5$. Thus, the first star forming sites are rare, but not yet so unlikely to render them completely irrelevant for cosmic history.

2.2. Virialization of DM Halos

Once a given perturbation becomes non-linear ($\delta_M \sim 1$), the corresponding dark matter (DM) collapses in on itself through a process of violent dynamical relaxation. The rapidly changing gravitational potential, $\partial\varphi/\partial t$, acts to scatter the DM particles, and their ordered motion is converted into random motion. The result of this “virialization” is a, roughly spherical, halo, where the kinetic and gravitational potential energies approach virial equilibrium: $2E_{\text{kin}} \simeq -E_{\text{pot}}$. Note that the total energy, $E_{\text{tot}} = E_{\text{kin}} + E_{\text{pot}} = -E_{\text{kin}}$, is negative, which implies that the halo is bound.

It is now convenient to define the gravitational potential (potential energy per unit mass), as follows:

$$\varphi = \frac{E_{\text{pot}}}{M_{\text{h}}} \simeq -\frac{GM_{\text{h}}}{R_{\text{vir}}} . \quad (4)$$

Here, M_{h} is the halo mass (gas + DM), which is connected to the halo density and radius, often called “virial” density and radius, via

$$M_{\text{h}} \simeq \frac{4\pi}{3} \rho_{\text{vir}} R_{\text{vir}}^3 . \quad (5)$$

The virial density, established after the virialization process is complete, is related to the background density of the universe at the time of collapse, at z_{vir} : $\rho_{\text{vir}} \simeq 200\bar{\rho}(z_{\text{vir}})$. In terms of the present-day background density, one has:

$$\bar{\rho}(z) = (1+z)^3 \bar{\rho}(z=0) = 2.5 \times 10^{-30} \text{ g cm}^{-3} (1+z)^3 . \quad (6)$$

A very useful concept to gauge how the baryonic (gaseous) component will behave when falling into the DM halos mentioned above is the “virial temperature”. The idea is to ask what would happen to a proton, of mass $m_{\text{H}} = 1.67 \times 10^{-24} \text{ g}$, when it is thrown into such a DM potential well. Through compressional heating, either adiabatically or involving shocks, the particle would acquire a random kinetic energy of:

$$k_{\text{B}} T_{\text{vir}} \simeq \epsilon_{\text{kin}} \simeq -\epsilon_{\text{pot}} \simeq \frac{GM_{\text{h}} m_{\text{H}}}{R_{\text{vir}}} , \quad (7)$$

where k_{B} is Boltzmann’s constant. Combining the equations above yields

$$T_{\text{vir}} \simeq 10^4 \text{ K} \left(\frac{M_{\text{h}}}{10^8 M_{\odot}} \right)^{2/3} \left(\frac{1+z_{\text{vir}}}{10} \right) , \quad (8)$$

where the normalizations are appropriate for a first-galaxy system, or, technically, and atomic cooling halo. For a minihalo, where $M_{\text{h}} \sim 10^6 M_{\odot}$ and $z_{\text{vir}} \sim 20$, one has: $T_{\text{vir}} \sim 1,000 \text{ K}$. A related quantity is the halo binding energy

$$E_{\text{b}} \simeq |E_{\text{tot}}| \simeq \frac{1}{2} \frac{GM_{\text{h}}^2}{R_{\text{vir}}} \simeq 10^{53} \text{ ergs} \left(\frac{M_{\text{h}}}{10^8 M_{\odot}} \right)^{5/3} \left(\frac{1+z_{\text{vir}}}{10} \right) , \quad (9)$$

where the normalizations are again appropriate for an atomic cooling halo. For a minihalo, the corresponding number is: $E_{\text{b}} \sim 10^{50} \text{ ergs}$. Comparing these values

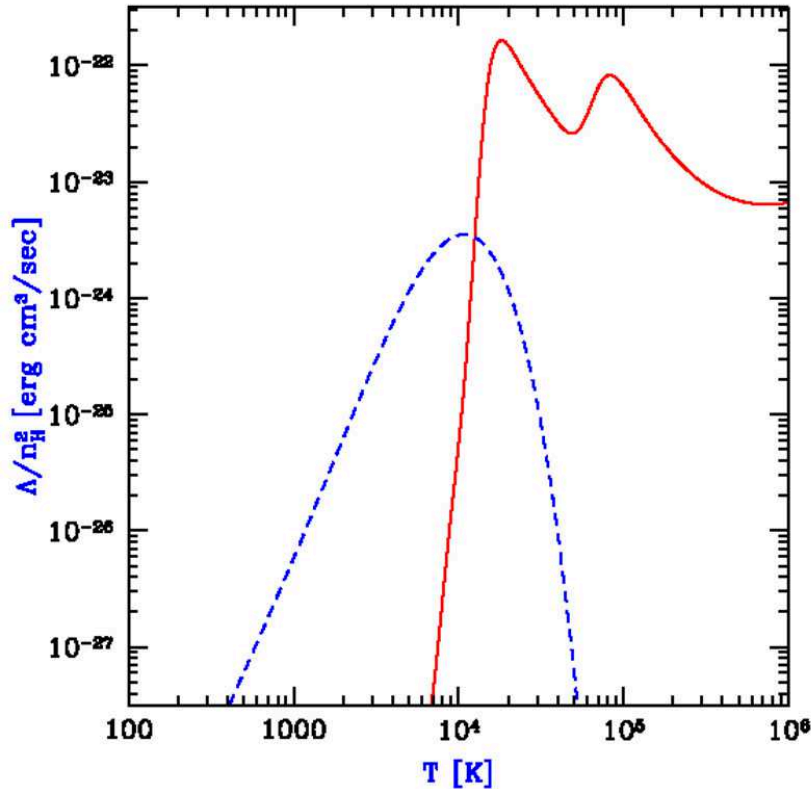


Figure 1. Cooling rate of primordial gas as a function of temperature. Shown is the contribution from atomic hydrogen and helium (*solid line*), as well as that from molecular hydrogen (*dashed line*). Atomic hydrogen line cooling is very efficient at temperatures of $T > 10^4$ K, whereas at lower temperatures, cooling has to rely on H_2 , which is a poor coolant. This is the regime of the minihalos, hosting the formation of the first stars. Adopted from Loeb (2010).

with the explosion energy of Pop III SNe, where $E_{\text{SN}} \simeq 10^{51} - 10^{52}$ ergs, one gets the zero-order prediction that minihalos may already be severely affected by SN feedback, evacuating most of the gas from the DM halo (see Ciardi & Ferrara 2005). The more massive atomic cooling halos, on the other hand, are expected to survive such negative SN feedback. This expectation is roughly born out by numerical simulations (see Bromm & Yoshida 2011).

2.3. Gas Dissipation

To form something interesting, such as stars, black holes, or galaxies, gas needs to be able to collapse to high densities. Initially, such collapse is triggered by the DM potential well in halos, as the DM is dynamically dominant, and the gas (the baryons) just follow along. However, different from DM, the gas is collisional, and therefore subject to compressional heating. If this heat could

not be radiated away, or dissipated, there would eventually be sufficient pressure support to stop the collapse. The key question then is: *Can the gas sufficiently cool?* A simple, but intuitively appealing and useful, answer is provided by the classical Rees-Ostriker-Silk criterion, that the cooling time has to be shorter than the free-fall time: $t_{\text{cool}} < t_{\text{ff}}$. If this criterion is fulfilled, a gas cloud will be able to condense to high densities, and possibly undergo gravitational runaway collapse. These important timescales are defined as follows: $t_{\text{ff}} \simeq 1/\sqrt{G\rho}$ and $t_{\text{cool}} \simeq nk_{\text{B}}T/\Lambda$, where Λ is the cooling function (in units of $\text{ergs cm}^{-3} \text{s}^{-1}$).

In Figure 1, the cooling function for primordial, pure H/He, gas is shown. One can clearly distinguish two distinct cooling channels, one at $T > 10^4 \text{ K}$, where cooling relies on atomic hydrogen lines, and one at lower temperatures, where the much less efficient H_2 molecule is the only available coolant. In the present-day interstellar medium (ISM), metal species would dominate cooling in this low-temperature regime, but, by definition, they are absent in the primordial universe. The first cooling channel governs the formation of the first galaxies (atomic cooling halos), since $T_{\text{vir}} \sim 10^4 \text{ K}$ for $M_{\text{h}} \sim 10^8 M_{\odot}$ and $z_{\text{vir}} \sim 10$. First star formation in minihalos, on the other hand, is governed by the low-temperature, H_2 , cooling channel. The reason is again that minihalos typically have $T_{\text{vir}} \sim 1,000 \text{ K}$.

2.4. Halo Angular Momentum

Another important ingredient for early star and galaxy formation is angular momentum. Current cosmological models posit that the post-recombination universe, at $z < 1,000$, was free of any circulation ($\nabla \times \vec{v} = 0$). Angular momentum is thought to have been created through tidal torques during the collapse of slightly asymmetric overdensities. The idea is that neighboring perturbations exert a net torque on a given halo, thus spinning it up. It is convenient to parameterize the resulting total angular momentum, J , of a virialized halo by a “spin parameter”:

$$\lambda \equiv \frac{J|E_{\text{tot}}|^{1/2}}{GM_{\text{h}}^{5/2}} \simeq \left(\frac{E_{\text{rot}}}{|E_{\text{tot}}|} \right)^{1/2}, \quad (10)$$

where $|E_{\text{tot}}|$ is again the total halo (binding) energy, and $E_{\text{rot}} \simeq J^2/(M_{\text{h}}R_{\text{vir}}^2)$ the total rotation energy. Numerical simulations, studying the large-scale evolution of the DM component, have shown that the spin parameter is distributed in a log-normal fashion with a mean of $\bar{\lambda} \simeq 0.04$ (see Mo et al. 2010).

For the DM component, the spin parameter is conserved during collisionless evolution. During the dissipational collapse of the gas, however, the spin parameter can change. In particular, the system can be driven towards centrifugal support, where $E_{\text{rot}} \simeq |E_{\text{tot}}|$. *What is the radius of centrifugal support?* Assume that the baryons collapse further, in a fixed DM halo potential. It is then straightforward to show that the baryons have to collapse by a factor of $\sim \lambda^{-1}$ to reach centrifugal support: $R_{\text{cent}} \simeq \lambda R_{\text{vir}}$. This then is the typical dimension of any large-scale disk that forms inside a dark matter halo.

3. First Star Formation: Basic Principles

Primordial star formation shares many similarities with the present-day case, in terms of basic principles. It is therefore always a good idea to seek guidance from the rich phenomenology and understanding reached in classical star formation theory (see McKee & Ostriker 2007; Zinnecker & Yorke 2007; Bodenheimer 2011 for reviews). In the following, in the spirit of our basic toolkit approach, we will address gravitational (Jeans) instability, the physics of protostellar accretion, and the properties of a generic stellar IMF.

3.1. Gravitational Instability

Consider a gaseous cloud of linear size L with a given mass density ρ and temperature T . Such a cloud will be unstable to gravitational runaway collapse, if: $t_{\text{sound}} > t_{\text{ff}}$, with $t_{\text{sound}} \simeq L/c_s$ being the sound-crossing time. The sound speed is $c_s \simeq \sqrt{k_B T / m_H} \propto T^{1/2}$. The intuition here is that the free-fall time measures the strength of gravity, in the sense that a smaller t_{ff} corresponds to a stronger force of gravity. Similarly, the sound-crossing timescale provides a measure for the strength of the opposing thermal pressure, where again a smaller t_{sound} indicates stronger pressure forces. The above timescale criterion for gravitational instability can be written as:

$$\frac{L}{c_s} > \frac{1}{\sqrt{G\rho}}. \quad (11)$$

This inequality defines the Jeans length

$$L > L_J \simeq \frac{c_s}{\sqrt{G\rho}}, \quad (12)$$

with the interpretation that a density perturbation has to exceed a certain critical size, such that gravitational forces take over, and cannot be balanced by thermal pressure any longer. One then defines the *Jeans mass*, as follows

$$M_J \sim \rho L_J^3 \simeq 500 M_\odot \left(\frac{T}{200 \text{ K}} \right)^{3/2} \left(\frac{n}{10^4 \text{ cm}^{-3}} \right)^{-1/2}, \quad (13)$$

where $n \simeq \rho/m_H$ is the hydrogen number density, and the normalizations reflect typical values in Pop III star forming regions. A closely related concept is the *Bonnor-Ebert mass*, where: $M_J \sim 2 \times M_{\text{BE}}$.

3.2. Protostellar Accretion

Every star, regardless of whether we are dealing with Pop I or Pop III, is assembled in an inside-out fashion, such that a small hydrostatic protostellar core is formed first at the center of a Jeans-unstable cloud. This initial core subsequently grows through accretion. Feedback effects from the growing protostar will eventually terminate this process, thus setting the final mass scale of the star. The initial core mass is small, close to the so-called *opacity limit for fragmentation*: $M_F \simeq 10^{-2} M_\odot$. This lower limit to the mass of a star can be derived by considering a cloud that is roughly in free-fall collapse. Collapse can proceed as long as the gas is able to radiate away the concomitant compressional heat. At

very high densities, however, the gas becomes opaque to this cooling radiation. Soon thereafter thermal pressure forces can stop the collapse, and a hydrostatic core is born. The key question now is to address the growth via accretion, which happens in two distinct regimes, first as predominantly spherical accretion, and then as disk-dominated accretion.

Spherical accretion For a roughly spherical gas cloud with a mass close to the Jeans mass, one can estimate the average accretion rate as follows:

$$\dot{M}_{\text{acc}} \sim \frac{M_{\text{J}}}{t_{\text{ff}}} \propto \frac{T^{3/2} \rho^{-1/2}}{\rho^{-1/2}} \sim T^{3/2} . \quad (14)$$

In the first step, we have assumed that gravity cannot move any material faster than the free-fall time. Using $c_s \propto T^{1/2}$, it is sometimes convenient to rewrite this as: $\dot{M} \simeq c_s^3/G$. Typically, one has for Pop I: $T \sim 10 \text{ K} \Rightarrow \dot{M} \sim 10^{-5} M_{\odot} \text{ yr}^{-1}$; and for Pop III: $T \sim 300 \text{ K} \Rightarrow \dot{M} \sim 10^{-3} M_{\odot} \text{ yr}^{-1}$. This two-order of magnitude difference in accretion rates is the basic physical reason why the first stars are believed to be more massive than present-day stars. Early on, protostellar accretion is mainly spherical, but with time, material with higher specific angular momentum (J/m) falls in, and results in the formation of a protostellar disk. The bulk of the accretion is then shifted to a disk mode.

Disk accretion Consider a circular shell, located at radius r , within a disk of surface mass density $\Sigma = M_{\text{disk}}/(\pi R_{\text{disk}}^2)$. For such a shell, one has

$$dM \simeq 2\pi r dr \Sigma . \quad (15)$$

Dividing by dt on both sides, yields the basic expression for the disk accretion rate: $\dot{M}_{\text{acc}} \simeq 2\pi r v_r \Sigma$, with $v_r = dr/dt$ being the radial (inflow) velocity. In a non-viscous disk, one would have: $v_r = 0$. Thus the reason that there is any infall is the presence of viscous shear forces, or, put differently, of friction. Such shear forces enable the outward transport of angular momentum, and the inward transport of mass.

Intuitively, to characterize viscous transport of linear momentum, one can set:

$$r v_r \sim \lambda_{\text{mfp}} \bar{v} \sim \nu , \quad (16)$$

with ν being the (kinematic) viscosity coefficient (in units of $\text{cm}^2 \text{ s}^{-1}$). The idea is that viscous transport involves the displacement of a particle (or fluid element) from a region of higher to lower momentum, e.g., a radial excursion in a Keplerian disk, where $v_{\text{rot}} \propto r^{-1/2}$. Such a displacement involves, on average, a distance equal to the mean-free path, λ_{mfp} , and proceeds with the average particle velocity, \bar{v} . The latter is often equal to the thermal velocity (or sound speed). It has long been realized that the molecular (microscopic particle) viscosity is much too small to have an effect on astrophysical systems, such as protostellar disks. Therefore, an “abnormal” source of viscosity is needed. Often, turbulent diffusion (transport) is implicated. Due to the inherent difficulties involved in the physics of turbulent transport, it is customary to employ the phenomenological α -prescription, introduced by Shakura & Sunyaev (1973): $\nu = \alpha H_p c_s$, where H_p is the pressure scale-height, effectively a measure of the vertical disk

height. The underlying intuition is that one is dealing with subsonic turbulence (else, for supersonic turbulence, shocks would rapidly dissipate any turbulent energy), such that: $\alpha < 1$. Note, that within this picture, the turbulent eddy size is bounded by the height of the disk, and the eddy turnover velocity by the sound speed. Also note that here, mesoscopic fluid elements (small compared to the total system, but large compared to individual atoms) have taken over the role of the individual atoms (or molecules) as fundamental carriers of linear momentum transport. From numerical simulations, we have the further constraint that, typically: $\alpha \simeq 10^{-2} - 1$, depending on the nature of the torques involved (gravitational, hydrodynamical, or magnetic).

We can now re-write our expression for the disk accretion rate in a form that can actually be evaluated in terms of easily accessible quantities:

$$\dot{M}_{\text{acc}} \simeq 2\pi\nu\Sigma. \quad (17)$$

The precise derivation would yield a “ 3π ” instead of our factor of 2π . Let us conclude this subsection by considering some numbers, typically encountered in Pop III disks (e.g., Clark et al. 2011): $\Sigma \sim 10^2 \text{ g cm}^{-2}$, $H_p \sim 100 \text{ AU} \sim 10^{15} - 10^{16} \text{ cm}$, and $c_s \sim 10^5 \text{ cm s}^{-1}$. Since here, angular momentum transport is dominated by gravitational torques, it is appropriate to choose $\alpha \sim 1$. We then estimate: $\dot{M}_{\text{acc}} \sim 10^{-3} - 10^{-2} M_{\odot} \text{ yr}^{-1}$. Accretion onto a massive star proceeds for roughly the Kelvin-Helmholtz timescale, $t_{\text{acc}} \sim t_{\text{KH}} \sim 10^5 \text{ yr}$, which in turn is the time it takes a (massive) star to reach the hydrogen-burning main sequence. One then has as a rough upper limit for the final mass of a Pop III star: $M_* \sim \dot{M}_{\text{acc}} t_{\text{acc}} \sim 100 M_{\odot}$. In reality, final masses will typically be smaller, since accretion may be terminated earlier on due to the negative radiative feedback from the growing protostar (e.g., Hosokawa et al. 2011; Stacy et al. 2012).

3.3. Initial Mass Function

The stellar IMF is a complicated function of mass, but it is often convenient to simply write it as a power law, valid for a given mass range. Specifically, one considers the number of stars per unit mass:

$$\frac{dN}{dM} \propto M^{-x}, \quad (18)$$

where the present-day IMF is characterized by the famous Salpeter slope of $x = 2.35$. To understand what the *typical* outcome of the star-formation process is, one can ask: *Where does most of the available mass go?* Or, put differently: What is the average stellar mass? This can be calculated as follows:

$$\bar{M} = \frac{\int_{M_{\text{low}}}^{M_{\text{up}}} M \frac{dN}{dM} dM}{\int_{M_{\text{low}}}^{M_{\text{up}}} \frac{dN}{dM} dM} = \frac{1-x}{2-x} \frac{M_{\text{up}}^{2-x} - M_{\text{low}}^{2-x}}{M_{\text{up}}^{1-x} - M_{\text{low}}^{1-x}} \sim 3.8 \times M_{\text{low}} \quad (19)$$

where in the last relation, we have used the Salpeter value for x , and M_{low} and M_{up} are the lower and upper mass limits, respectively. In general, one can neglect all terms involving M_{up} above, as long as $x > 2$. This means that a Salpeter-like IMF is dominated by the lower-mass limit. For Pop I (present-day) stars, one often takes $M_{\text{low}} \simeq 0.1 M_{\odot}$ and $M_{\text{up}} \simeq 100 M_{\odot}$, such that $\bar{M} \sim 0.5 M_{\odot}$,

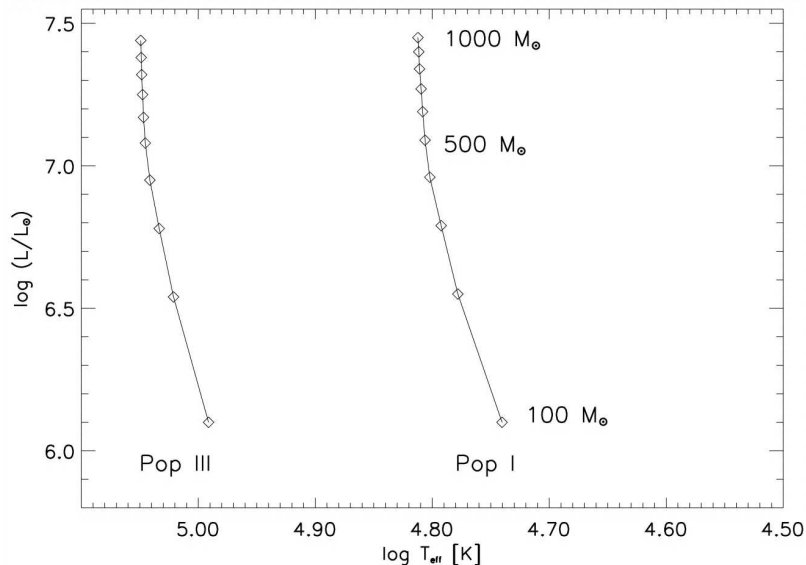


Figure 2. Zero-age main sequence (ZAMS) for very massive stars. Shown is a comparison between the Pop III (*left line*) and Pop I cases (*right line*). Stellar luminosity (in units of L_{\odot}) is plotted vs. effective temperature (in K). *Diamond-shaped symbols*: Stellar masses along the sequence, from $100M_{\odot}$ (bottom) to $1000M_{\odot}$ (top). As can be seen, the Pop III ZAMS is shifted to higher values of effective temperature, asymptotically reaching $T_{\text{eff}} \simeq 10^5$ K. Note that current estimates for the Pop III mass are somewhat less extreme. Adopted from Bromm et al. (2001).

whereas for Pop III, current theory postulates a characteristic (typical) mass of $\bar{M} \sim 4M_{\text{low}} \sim \text{a few} \times 10M_{\odot}$, assuming that the Pop III IMF were to exhibit a slope similar to Salpeter. The latter assumption is not at all proven, and just serves as a zero-order guess.

4. First Stars: Basic Properties

In the following, we will address the fundamentals of the structure and evolution of massive, Pop III stars. Many of these relations are strictly valid only for stars with $M_* > 100M_{\odot}$. The stellar physics in this high-mass regime, although involving extreme energies and temperatures, is of an appealing simplicity. Recent simulations have revised the Pop III mass-scale downwards to more modest values ($M_* \sim 10 - 50M_{\odot}$), but the simple high-mass physics nevertheless provides us with very useful order-of-magnitude estimates. The discussion here is largely based on Bromm et al. (2001), and we refer the reader to this paper, and references therein, for a more detailed (numerical) treatment.

In this spirit, we start by assuming a typical Pop III stellar mass of $M_* \sim 100M_{\odot}$. Massive stars are dominated by radiation pressure (see below), and

their structure can therefore approximately be described as a polytrope with index $n = 3$. For such a configuration, one can derive the following mass-radius relation:

$$R_* \simeq 5R_\odot \left(\frac{M_*}{100M_\odot} \right)^{1/2}, \quad (20)$$

which is valid for a star on the hydrogen-burning main sequence. It is then straightforward to estimate the average mass: $\langle \rho \rangle = M_*/(4\pi/3R_*^3) \sim 1 \text{ g cm}^{-3}$, which is of the same order as for the Sun. Somewhat surprisingly, massive stars, therefore do not involve extreme densities. We next wish to estimate the temperature, both at the surface and in the deep interior. To accomplish this, one has to consider the pressure inside the star.

4.1. Radiation Pressure

In massive stars ($M_* > 50M_\odot$), radiation pressure starts to be important, compared with the usual gas (thermal) pressure. For ultra-relativistic particles, in our case photons, one has the general relation between pressure and energy density (in units of erg cm^{-3}): $P_{\text{rad}} = 1/3 u_{\text{rad}}$. The latter is given by the Stefan-Boltzmann law:

$$u_{\text{rad}} = \frac{8\pi^5}{15} \frac{k_B^4}{h^3 c^3} T^4 = a_{\text{rad}} T^4, \quad (21)$$

where h is Planck's constant. The radiation constant has the numerical value: $a_{\text{rad}} = 7.57 \times 10^{-15} \text{ erg K}^{-4} \text{ cm}^{-3}$. Thus, we can write the radiation (photon) pressure, as:

$$P_{\text{rad}} = \frac{1}{3} a_{\text{rad}} T^4. \quad (22)$$

4.2. Hydrostatic Equilibrium

The motion of any fluid element in a star is governed by the Euler equation:

$$\rho \frac{D\vec{v}}{Dt} = -\nabla P + \rho \vec{g}, \quad (23)$$

where D/Dt is the substantial (moving with the fluid) derivative, and \vec{g} the gravitational acceleration. Assuming spherical symmetry and $D/Dt = 0$, we get the equation of hydrostatic equilibrium, which is crucial for the structure of stars:

$$\frac{dP_{\text{rad}}}{dr} = -\rho \frac{Gm}{r^2}, \quad (24)$$

Here, we have assumed $P = P_{\text{gas}} + P_{\text{rad}} \sim P_{\text{rad}}$, as is appropriate for massive stars. Above, we introduce the Lagrangian mass coordinate, $m = m(r)$, which measures the total mass contained within a shell of radius r . We now re-work this equation in an order-of-magnitude fashion:

$$\frac{a_{\text{rad}} T^4}{R_*} \simeq \langle \rho \rangle \frac{GM_*}{R_*^2}, \quad (25)$$

resulting in an estimate for the typical interior temperature in a massive Pop III star:

$$T_I = \left(\frac{\langle \rho \rangle}{a_{\text{rad}}} \frac{GM_*}{R_*} \right)^{1/4} \sim 10^8 \text{ K}. \quad (26)$$

The next question is: *How is this related to the surface temperature?* In addressing it, we need to consider how energy is transported in the stellar interior via photon diffusion.

4.3. Radiative Diffusion

Let us begin with a thought experiment. For the moment, (wrongly) assume that photons are free to escape from the hot interior of a star, which would imply negligible opacity (i.e., the capability of stellar gas to bottle-up radiation). The timescale for such hypothetical, direct escape would be: $t_{\text{direct}} = R_*/c$. Within the same setup, we would estimate the stellar luminosity as follows:

$$L = \frac{\Delta E}{\Delta t} \sim \frac{u_{\text{rad}} R_*^3}{t_{\text{direct}}} \simeq \frac{a_{\text{rad}} c T_I^4 R_*^3}{R_*} \simeq a_{\text{rad}} c R_*^2 T_I^4. \quad (27)$$

The radiation constant is related to the Stefan-Boltzmann constant via: $a_{\text{rad}} = 4\sigma_{\text{SB}}/c$, where: $\sigma_{\text{SB}} = 5.67 \times 10^{-5} \text{ erg s}^{-1} \text{ cm}^{-2} \text{ K}^{-4}$. We can thus re-phrase the equation above in a form similar to the standard blackbody expression:

$$L = 4\pi R_*^2 \sigma_{\text{SB}} T_I^4. \quad (28)$$

Now, why is this reasoning incorrect? The answer is that in reality photons are trapped inside a star. Indeed, stellar material is typically extremely opaque to radiation, such that the photons engage in a very slow diffusion process, and eventually leak out from a narrow layer close to the surface, the stellar photosphere. Effectively, we are dealing with a near-blackbody, characterized by an effective (photospheric) temperature, T_{eff} . If we further replace the (incorrect) direct escape timescale with the (correct) diffusion time, we have:

$$L = \frac{\Delta E}{\Delta t} \simeq \frac{\Delta E}{t_{\text{diff}}} = 4\pi R_*^2 \sigma_{\text{SB}} T_{\text{eff}}^4, \quad (29)$$

such that:

$$T_{\text{eff}} \simeq \left(\frac{t_{\text{direct}}}{t_{\text{diff}}} \right)^{1/4} T_I. \quad (30)$$

Our remaining task is therefore to estimate the diffusion timescale.

We can do this by modeling diffusion as a (nearly-isotropic) random walk. If l_γ is the photon mean-free path, and N_{sc} the number of scatterings needed for a photon to escape from the star, basic random-walk theory yields: $R_* = \sqrt{N_{\text{sc}}} l_\gamma$. Stellar material is extremely opaque, and one typically has: $l_\gamma \simeq 1/(n\sigma_{\text{T}}) \simeq 1 \text{ cm}$. Here, we have assumed that the opacity is dominated by electron (Thomson) scattering, with an interaction cross-section of $\sigma_{\text{T}} = 0.67 \times 10^{-24} \text{ cm}^2$. The diffusion timescale can then be estimated via:

$$t_{\text{diff}} \simeq \frac{N_{\text{sc}} l_\gamma}{c} \simeq \frac{R_*^2}{l_\gamma c}. \quad (31)$$

Combining everything, we finally get:

$$T_{\text{eff}} \simeq \left(\frac{l_\gamma}{R_*} \right)^{1/4} T_I \sim 10^{-3} T_I \sim 10^5 \text{ K}. \quad (32)$$

Massive Pop III stars are thus extremely hot (compare to the solar $T_{\text{eff},\odot} \simeq 6,000\text{ K}$), which in turn implies a number of key consequences for early cosmic history. Among them is a very high specific (per unit stellar mass) production rate of ionizing photons. It is useful to remember: $\dot{N}_{\text{ion}} \simeq 10^{48} \text{ s}^{-1} M_{\odot}^{-1}$. In addition, such hot stars can also produce copious amounts of He-ionizing photons, including those required for the second ionization of He (54 eV). Normally, such extremely energetic radiation is not produced by stars, and instead originates in quasar (accreting black-hole) sources.

4.4. Stellar Luminosity

Combining the expressions above, we find for the Pop III stellar luminosity:

$$L = 4\pi R_*^2 \sigma_{\text{SB}} T_{\text{eff}}^4 \simeq 10^6 L_{\odot} \left(\frac{M_*}{100 M_{\odot}} \right). \quad (33)$$

To repeat, in deriving this, we have assumed that: (i) pressure is dominated by radiation (appropriate for all massive stars), and (ii) opacity is dominated by Thomson scattering (appropriate for metal-free stars). The $L \propto M_*$ scaling is characteristic for very massive stars. Indeed, the luminosity for massive Pop III stars is close to the theoretical upper limit, the so-called “Eddington luminosity”.

The Eddington limit can be derived by demanding that the radiation pressure associated with a given luminosity does not exceed the force of gravity. Specifically, let us consider the balance of forces exerted on a combination of one proton and one electron, where the proton provides (most of) the mass, and the (free) electron the opacity (via Thomson scattering):

$$\frac{G m_{\text{H}} M_*}{r^2} \simeq \frac{\Delta p_{\gamma}}{\Delta t}, \quad (34)$$

where Δp_{γ} is the absorbed photon momentum per particle:

$$\frac{\Delta p_{\gamma}}{\Delta t} = \frac{\Delta E_{\gamma}/c}{\Delta t} = \frac{1}{c} \frac{L}{4\pi r^2} \sigma_{\text{T}}. \quad (35)$$

Thus, one has $L < L_{\text{EDD}}$, where the Eddington luminosity is:

$$L_{\text{EDD}} = \frac{4\pi G m_{\text{H}}}{\sigma_{\text{T}}} M_* = 1.3 \times 10^{38} \text{ erg s}^{-1} \left(\frac{M_*}{M_{\odot}} \right). \quad (36)$$

This is very close to the estimate in equation (33), demonstrating that $L \sim L_{\text{EDD}}$ for very massive ($M_* > 100 M_{\odot}$) Pop III stars. Again, these relations still give reasonable ballpark numbers for less extreme masses.

In Figure 2, the Pop III zero-age main sequence (ZAMS) is shown, together with the comparison Pop I sequence, in both cases for very massive stars. As is evident there, the effective temperatures asymptotically approach constant values, $T_{\text{eff}} \sim 10^5 \text{ K}$ for Pop III, and $\sim 60,000 \text{ K}$ for Pop I. Luminosities, however, are very similar for a star of given mass, regardless of metallicity. The reason that Pop III stars are so much hotter (bluer) is their much more compact configuration, which is in turn a reflection of the reduced opacity in the outer envelope.

Finally, let us estimate the lifetime of massive Pop III stars. Assuming that such stars radiate close to the Eddington limit, and that they are almost fully convective, one has the simple relation:

$$t_* \simeq \frac{0.007 M_* c^2}{L_{\text{EDD}}} \simeq 3 \times 10^6 \text{ yr}, \quad (37)$$

where the factor of 0.007 is the efficiency of hydrogen burning. These are very short lifetimes, compared with the solar $t_{*,\odot} \sim 10^{10}$ yr. The implication is that any feedback effects exerted on the surrounding IGM by the Pop III star are almost instantaneous. For example, the pristine gas in the neighborhood of the Pop III star is rapidly converted into metal-enriched material, such that any subsequent round of star formation will already lead to Pop II stars. Also note that for very massive stars the stellar lifetime becomes independent of mass.

5. First Galaxy Assembly

With the emergence of the first galaxies, we witness the onset of supersonic turbulence, which is expected to have important consequences for star formation (reviewed in Mac Low & Klessen 2004; McKee & Ostriker 2007). To see this, we estimate the Reynolds and Mach numbers, as follows. The Reynolds number measures the relative importance of inertia and viscous forces:

$$Re = \frac{\text{inertial acceleration}}{\text{viscous acceleration}} \simeq \frac{\frac{V}{T}}{\nu \frac{V}{L^2}} \simeq \frac{VL}{\nu}, \quad (38)$$

where V , L , $T = L/V$ are characteristic velocity, length, and time scales, respectively. For the first galaxies, we can estimate: $V \sim v_{\text{vir}} \sim 10 \text{ km s}^{-1}$, $L \sim R_{\text{vir}} \sim 1 \text{ kpc}$, and $\nu \sim \lambda_{\text{mfp}} c_s \sim 10^{18} \text{ cm}^2 \text{ s}^{-1}$. For the last estimate, we have assumed: $\lambda_{\text{mfp}} = 1/(n\sigma_{\text{coll}}) \sim 10^{13} \text{ cm}$, if the number density is typically $n \sim 10^3 \text{ cm}^{-3}$, and we consider collisions between neutral hydrogen atoms ($\sigma_{\text{coll}} \sim 10^{-16} \text{ cm}^2$). For the typical particle velocity, we assume the sound-speed of H_2 -cooled gas ($c_s \sim 1 \text{ km s}^{-1}$). The Reynolds number in the center of the first galaxies is therefore: $Re \sim 10^9$, indicating a highly-turbulent situation. The Mach number is: $Ma \sim V/c_s \sim v_{\text{vir}}/c_s \sim 10$, indicating supersonic flows.

Supersonic turbulence generates density fluctuations in the ISM. Statistically, these can be described with a log-normal probability density function (PDF):

$$f(x)dx = \frac{1}{\sqrt{2\pi\sigma_x^2}} \exp\left[-\frac{(x - \mu_x)^2}{2\sigma_x^2}\right] dx, \quad (39)$$

where $x \equiv \ln(\rho/\bar{\rho})$, and μ_x and σ_x^2 are the mean and dispersion of the distribution, respectively. The latter two are connected: $\mu_x = -\sigma_x^2/2$. This relation can easily be derived by interpreting the PDF above as a distribution (of x) by volume. One then has for the volume-averaged density: $\bar{\rho} = \int \rho f(x)dx = \bar{\rho} \int e^x f(x)dx$, which yields the desired result. Numerical simulations have shown that the dispersion of the density PDF is connected to the Mach number of the flow: $\sigma_x^2 \simeq \ln(1 + 0.25Ma^2)$. Inside the first galaxies, one finds values close to $\sigma_x \simeq 1$.

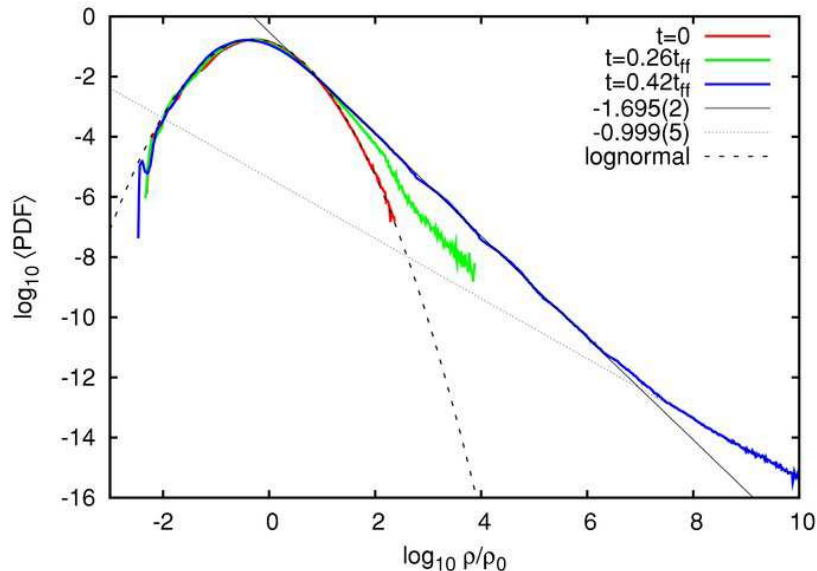


Figure 3. Density distribution in supersonically-turbulent flows. Initially ($t = 0$), the density PDF is log-normal. With time, a pronounced power-law tail develops towards high density. This is a reflection of the gas self-gravity. Adopted from Kritsuk et al. (2011).

In Figure 3, we show an illustrative example from a numerical simulation of isothermal, supersonic turbulence. There, it is also evident that the self-gravity of the gas imprints a power-law tail toward the highest densities, on top of the log-normal PDF at lower densities, which is generated by purely hydrodynamical effects.

6. Observational Signature

It is useful to recall the derivations of some of the key quantities in observational cosmology, specifically luminosity and angular-diameter distance, as well as the observed flux. It is also useful to assemble estimates for their typical values as encountered in the first galaxies. Further details are given in the monographs mentioned above. In addition, a comprehensive survey of high-redshift galaxy observations, including a description of the key methods and tools, is given by Appenzeller (2009).

6.1. Cosmological Distances

In analogy to the usual inverse-square law, the luminosity distance, d_L , is defined via:

$$f_{\text{obs}} = \frac{\Delta E_{\text{obs}}}{\Delta t_{\text{obs}} \Delta A_{\text{obs}}} = \frac{L_{\text{em}}}{4\pi d_L^2}, \quad (40)$$

where here and in the following we refer to quantities that are measured at $z = 0$ with the subscript “obs”, and with “em” to source-frame quantities (emitted at a given redshift z). Note that: $\Delta E_{\text{obs}} = \Delta E_{\text{em}}/(1+z)$, and $\Delta t_{\text{obs}} = \Delta t_{\text{em}}(1+z)$ relate small differences in energy and time in the two frames. To evaluate ΔA_{obs} , carry out the following thought experiment: Imagine that you could somehow ‘step outside’ our universe, looking down at the scene from some (higher-dimensional) bird’s-eye perspective. Such a perspective, which of course is completely inaccessible in practice, would allow you to measure distances, *as they would appear today*. Or, put differently, you somehow managed to stop the expansion of the universe, keep everything frozen at $z = 0$, and go about measuring the distance, with some appropriate measuring rod, from the observer (the telescope) to where the source would be located today. Recall that the source was much closer when it emitted the photon that we receive today, but has hence receded due to cosmic expansion. This source-observer distance, $r(z)$, is called *comoving distance*, or *proper distance*. Although it cannot be directly measured, but instead can only be calculated by assuming a theoretical model of the universe, this concept is nevertheless extremely useful in cosmology. Assuming a point source at a given redshift z , we can now write the (proper) size of the spherical surface over which the photons have been spread, as: $\Delta A_{\text{obs}} = 4\pi r^2(z)$.

To calculate the comoving distance, consider the Robertson-Walker (RW) metric:

$$ds^2 = c^2 dt^2 - a^2 dr^2, \quad (41)$$

where we have assumed a spatially flat universe, and where ds is the (invariant) space-time interval. Since they travel along null geodesics ($ds = 0$), one has for photons: $dr = c dt/a$ (recall $a = 1/(1+z)$). The RW metric describes any homogeneous, isotropic, and expanding universe. To fully specify the background cosmological model, we also need the Friedmann equation, governing \dot{a} . The latter can in turn be derived from the Einstein field equations of general relativity (see Mo et al. 2010), yielding:

$$\left(\frac{\dot{a}}{a}\right) = H(z) = H_0 \sqrt{\Omega_m(1+z)^3 + \Omega_\Lambda}, \quad (42)$$

where H_0 , Ω_m , and Ω_Λ are the Hubble constant, the density parameter for matter, and that for dark energy, respectively, as measured to very high precision by *WMAP* (Komatsu et al. 2011). In this expression, we again assume a spatially flat universe (zero curvature). We can now carry out the integration along the photon-geodesic:

$$r(z) = c \int_0^z (1+z') \left| \frac{dt}{dz'} \right| dz' = \frac{c}{H_0} \int_0^z \frac{dz'}{\sqrt{\Omega_m(1+z')^3 + \Omega_\Lambda}}, \quad (43)$$

where we use the Friedmann equation in the last step.

We have now all the ingredients in hand to find an expression for the luminosity distance:

$$f_{\text{obs}} = \frac{1}{4\pi(1+z)^2 r^2} \frac{\Delta E_{\text{em}}}{\Delta t_{\text{em}}} = \frac{L_{\text{em}}}{4\pi r^2(1+z)^2}. \quad (44)$$

Comparing with the definition above, we finally have: $d_L(z) = (1+z)r(z)$. It is useful to memorize the ballpark number for a source at $z \simeq 10$, appropriate for the first galaxies: $d_L(z) \sim 10^2$ Gpc.

Next, let us derive the analogous expression for *angular-diameter distance*, d_A , where we again start with a definition that follows basic, geometrical intuition. If a source at z , having a true (proper) transverse size of D , is observed to have an apparent angular size of Θ , we define: $\Theta = D/d_A$. And let us again assume our bird's-eye perspective, as before. How would the source appear at the present-day ($z = 0$), if it had just been coasting along with the expanding universe since the time that the photons, reaching us now, were originally emitted? The situation can be described with a virtual triangle, where:

$$\Theta = \frac{D(1+z)}{r(z)} = \frac{D}{d_A}, \quad (45)$$

giving us our result: $d_A = r(z)/(1+z)$. Note that the two fundamental distances of observational cosmology are connected: $d_L = d_A(1+z)^2$, such that it suffices to remember only one. For a first galaxy, where $D \sim 1$ kpc, one finds: $\Theta \sim D/d_A \sim 1 \text{ kpc}/1 \text{ Gpc} \sim 10^{-6} \sim 0.2''$. The near-IR camera on-board the *JWST* (NIRCam) should thus be able to marginally resolve these sources.

6.2. Observed Fluxes

To estimate how bright a first galaxy is likely to be, we need to consider the observed specific flux (flux per unit frequency):

$$f_{\nu,\text{obs}} = \frac{\Delta E_{\text{obs}}}{\Delta t_{\text{obs}} \Delta A_{\text{obs}} \Delta \nu_{\text{obs}}} = \frac{\Delta E_{\text{em}}/(1+z)}{4\pi r^2 \Delta t_{\text{em}} \Delta \nu_{\text{em}}} \simeq (1+z) \frac{L_{\nu,\text{em}}}{4\pi d_L^2}. \quad (46)$$

To arrive at a zeroth-order guess, we assume that the total stellar mass involved in the starburst at the center of a first galaxy is: $M_* \sim 10^5 M_\odot$. If we further assume that we are dealing with a top-heavy Pop III burst, the stellar radiation will be characterized by $T_{\text{eff}} \sim 10^5$ K, corresponding to a peak frequency of $\nu_{\text{max}} \sim 10^{16}$ Hz, and a total luminosity close to the Eddington-luminosity (see Section 4): $L \sim L_{\text{EDD}} \sim 10^{43} \text{ erg s}^{-1}$. The emitted specific luminosity is thus: $L_{\nu,\text{em}} \sim L_{\text{EDD}}/\nu_{\text{max}} \sim 10^{27} \text{ erg s}^{-1} \text{ Hz}^{-1}$. The observed (specific) flux for a first galaxy at $z \sim 10$ is then:

$$f_{\nu,\text{obs}} \sim 10^{-32} \text{ erg s}^{-1} \text{ cm}^{-2} \text{ Hz}^{-1} = 1 \text{ nJy}. \quad (47)$$

The nJy is indeed the typical brightness level that the *JWST* is designed to image with NIRCam, thus reiterating the point that with this next-generation facility, we will get the first galaxies within reach of deep-field exposures.

7. Outlook

The next decade will be very exciting as we are opening up multiple windows into the cosmic dark ages. We will finally be able to close the remaining gap in the long quest to reconstruct the entire history of the universe, which began with the

pioneers of cosmology in the 1920s. There will be many opportunities to make important discoveries, e.g., in directly detecting the first sources of light, and in working out a well-tested theoretical framework for star and galaxy formation at the dawn of time. Very likely, serendipity will play a crucial role. It is thus a good idea to equip oneself with a comprehensive set of tools, such as the basic physics covered in these lecture notes. After all, there is wisdom to the old adage that “fortune favors the prepared mind”.

Acknowledgments. I would like to thank the organizers for their warm hospitality, and for putting together a stimulating program. VB acknowledges support from NSF grant AST-1009928 and NASA ATRP grant NNX09AJ33G.

References

- Appenzeller, I. 2009, *High-Redshift Galaxies* (Berlin: Springer)
- Barkana, R., Loeb, A. 2001, *Physics Reports*, 349, 125
- Beers, T. C., Christlieb, N. 2005, *ARA&A*, 43, 531
- Bloom, J. S. 2011, *What are Gamma-ray Bursts?* (Princeton: Princeton Univ. Press)
- Bodenheimer, P. H. 2011, *Principles of Star Formation* (Berlin: Springer)
- Bromm, V., Kudritzki, R. P., Loeb, A. 2001, *ApJ*, 552, 464
- Bromm, V., Larson, R. B. 2004, *ARA&A*, 42, 79
- Bromm, V., Yoshida, N., Hernquist, L., McKee, C. F. 2009, *Nature*, 459, 49
- Bromm, V., Yoshida, N. 2011, *ARA&A*, 49, 373
- Ciardi, B., Ferrara, A. 2005, *Space Science Reviews*, 116, 625
- Clark, P. C., Glover, S. C. O., Smith, R. J., et al. 2011, *Science*, 331, 1040
- Frebel, A., Johnson, J. L., Bromm, V. 2007, *MNRAS*, 380, L40
- Frebel, A. 2010, *Astronomische Nachrichten*, 331, 474
- Freeman, K., Bland-Hawthorn, J. 2002, *ARA&A*, 40, 487
- Furlanetto, S. R., Oh, S. P., Briggs, F. H. 2006, *Physics Reports*, 433, 181
- Gardner, J. P., Mather, J. C., Clampin, M., et al. 2006, *Space Science Reviews*, 123, 485
- Glover, S. C. O. 2005, *Space Science Reviews*, 117, 445
- Greif, T. H., Springel, V., White, S. D. M., et al. 2011, *ApJ*, 737, 75
- Hosokawa, T., Omukai, K., Yoshida, N., Yorke, H. W. 2011, *Science*, 334, 1250
- Karlsson, T., Bromm, V., Bland-Hawthorn, J. 2012, *Rev. Mod. Phys.*, submitted (arXiv:1101.4024)
- Komatsu, E., Smith, K. M., Dunkley, J., et al. 2011, *ApJS*, 192, 18
- Kouveliotou, C., Woosley, S. E., Wijers, R. A. M. J. (eds.) 2012, *Gamma-ray Bursts* (Cambridge: Cambridge Univ. Press)
- Kritsuk, A. G., Norman, M. L., Wagner, R. 2011, *ApJ*, 727, L20
- Loeb, A. 2010, *How did the First Stars and Galaxies Form?* (Princeton: Princeton Univ. Press)
- Mac Low, M. M., Klessen, R. S. 2004, *Rev. Mod. Phys.*, 76, 125

- McKee, C. F., Ostriker, E. C. 2007, *ARA&A*, 45, 565
- Mo, H., Van den Bosch, F., White, S. D. M. 2010, *Galaxy Formation and Evolution* (Cambridge: Cambridge Univ. Press)
- Oh, S. P., Haiman, Z. 2002, *ApJ*, 569, 558
- Salvadori, S., Ferrara, A. 2009, *MNRAS*, 395, L6
- Shakura, N. I., Sunyaev, R. A. 1973, *A&A*, 24, 337
- Stacy, A., Greif, T. H., Bromm, V. 2010, *MNRAS*, 403, 45
- Stacy, A., Greif, T. H., Bromm, V. 2012, *MNRAS*, in press (arXiv:1109.3147)
- Stiavelli, M. 2009, *From First Light to Reionization: The End of the Dark Ages* (Weinheim: Wiley-VCH)
- Turk, M. J., Abel, T., O'Shea, B. 2009, *Science*, 325, 601
- Whalen, D. J., Bromm, V., Yoshida, N. (eds.) 2010, *The First Stars and Galaxies: Challenges for the Next Decade* (AIP Conference Series, vol. 1294)
- Zinnecker, H., Yorke, H. W. 2007, *ARA&A*, 45, 481